Osteopenia, decreased bone formation and impaired osteoblast development in *Sox4* heterozygous mice

Lise Sofie Haug Nissen-Meyer[1,*], Rune Jemtland[2], Vigdis T. Gautvik[1], Mona E. Pedersen[1], Rita Paro[1,‡], Dario Fortunati[1], Dominique D. Pierroz[3], Vincent A. Stadelmann[4], Sjur Reppe[1], Finn P. Reinholt[5], Andrea Del Fattore[6], Nadia Rucci[6], Anna Teti[6], Serge Ferrari[3] and Kaare M. Gautvik[1,7,§]

[1]Department of Biochemistry, Institute of Basic Medical Sciences, University of Oslo, N-0317 Oslo, Norway
[2]Endocrine Section, Department of Medicine, University of Oslo, Rikshospitalet-Radiumhospitalet Medical Centre, N-0027 Oslo, Norway
[3]Service of Bone Diseases, WHO Collaborating Center for Osteoporosis Prevention, Geneva University Hospital, 1211 Geneva, Switzerland
[4]Laboratory of Biomechanical Orthopedics, EPFL-HOSR, Ecole Polytechnique Fédérale de Lausanne, 1015 Lausanne, Switzerland
[5]Institute of Pathology, University of Oslo, and The Pathology Clinic, Rikshospitalet-Radiumhospitalet Medical Centre, N-0027 Oslo, Norway
[6]Department of Experimental Medicine, University of L'Aquila, 67100 L'Aquila, Italy
[7]Department of Clinical Chemistry, Ullevål University Hospital, N-0407 Oslo, Norway
*Present address: The Biotechnology Centre of Oslo, University of Oslo, N-0317 Oslo, Norway
‡Present address: Department of Biomedical Sciences and Technologies, University of L'Aquila, 67100 L'Aquila, Italy
§Author for correspondence (e-mail: k.m.gautvik@medisin.uio.no)

Accepted 11 June 2007
Journal of Cell Science 120, 2785-2795 Published by The Company of Biologists 2007
doi:10.1242/jcs.003855

Summary

The transcription factor Sox4 is vital for fetal development, as *Sox4*$^{-/-}$ homozygotes die in utero. *Sox4* mRNA is expressed in the early embryonic growth plate and is regulated by parathyroid hormone, but its function in bone modeling/remodeling is unknown. We report that *Sox4*$^{+/-}$ mice exhibit significantly lower bone mass (by dual-energy X-ray absorptiometry) from an early age, and fail to obtain the peak bone mass of wild-type (WT) animals. Microcomputed tomography (μCT), histomorphometry and biomechanical testing of *Sox4*$^{+/-}$ bones show reduced trabecular and cortical thickness, growth plate width, ultimate force and stiffness compared with WT. Bone formation rate (BFR) in 3-month-old *Sox4*$^{+/-}$ mice is 64% lower than in WT. Primary calvarial osteoblasts from *Sox4*$^{+/-}$ mice demonstrate markedly inhibited proliferation, differentiation and mineralization. In these cultures, osterix (*Osx*) and osteocalcin (*OCN*) mRNA expression was reduced, whereas *Runx2* mRNA was unaffected. No functional defects were found in osteoclasts. Silencing of *Sox4* by siRNA in WT osteoblasts replicated the defects observed in *Sox4*$^{+/-}$ cells. We demonstrate inhibited formation and altered microarchitecture of bone in *Sox4*$^{+/-}$ mice versus WT, without apparent defects in bone resorption. Our results implicate the transcription factor Sox4 in regulation of bone formation, by acting upstream of Osx and independent of Runx2.

Supplementary material available online at
http://jcs.biologists.org/cgi/content/full/120/16/2785/DC1

Key words: Sox4, Bone density, Bone biomechanics, Bone formation rate, Osteoblast cultures, Osteoblast function

Introduction

Bone mineral density (BMD) is considered an important determinant for bone strength and fracture risk in human bone disorders. Bones are renewed throughout life through bone remodeling, i.e. synthesis of bone matrix by osteoblasts (of mesenchymal origin) and bone resorption by osteoclasts (of hematopoietic origin) (Jilka, 2003). In osteoporosis, perturbations in local cytokines, growth factors, systemic hormones and transcription factors cause imbalance between bone formation and resorption, resulting in net bone loss (Karsenty, 1999). Peak bone mass, the result of net bone accrual in early life and with a maximum in the second and third decade of life, is greatly influenced by genetic factors (50-85%) (Giguere and Rousseau, 2000; Ralston, 2002; Nguyen et al., 2003; Ralston and de Crombrugghe, 2006). BMD depends on peak bone mass, but also on the rate of bone loss in later life. Although polymorphisms of several genes associated with reduced bone mass and increased fracture risk have been identified, e.g. bone morphogenetic protein-2 (*BMP-2*), *LRP5* and *Collagen I* (Grant et al., 1996; Johnson et al., 2004; Mundy, 2006; Ralston, 2002), the mechanisms controlling the variation of bone loss rate are mostly unknown.

In skeletal tissue, mesenchymal bone cell development from a common progenitor cell (Pittenger et al., 1999) is under transcriptional regulation: Runx2 and osterix (Osx) (Ducy, 2000; Nakashima et al., 2002) are crucial for normal osteogenesis, whereas Sox5, Sox6 and Sox9 (Lefebvre et al., 1998) and PPARγ ligands (Lecka-Czernik et al., 2002) influence chondrocyte and adipocyte development, respectively. Several transcription factors in the Sox family [related to sex-determining region Y (SRY) proteins] are involved in skeletal development in addition to their roles in developmental processes in other tissues (Schilham et al., 1996; Hong and Saint-Jeannet, 2005). Sox4 contains the Sox family characteristic high mobility group (HMG) box, and is highly conserved in human, mouse, chicken (Maschhoff et al., 2003) and fish (Hett and Ludwig, 2005; Mavropoulos et al., 2005), and expressed in brain, gonads, lung, heart and thymus (Schilham et al., 1996). It is implicated in lymphocyte differentiation (Schilham et al., 1997; van de Wetering et al.,

1993), cancer (Liu et al., 2006; Pramoonjago et al., 2006) and apoptosis (Ahn et al., 2002; Hur et al., 2004; Pramoonjago et al., 2006).

Our group first reported expression of Sox4 in skeletal tissue; *Sox4* mRNA is highly expressed in normal and clonal osteoblasts of human and rat origin, where it is stimulated by parathyroid hormone (PTH), and the transcript is predominantly localized in hypertrophic chondrocytes in developing mouse hindlimbs (Reppe et al., 2000). We recently demonstrated elevated *SOX4* mRNA levels in bone biopsies from patients with active primary hyperparathyroidism compared with levels after successful surgery and PTH normalization (Reppe et al., 2006). Sekiya et al. demonstrated that induction of chondrogenesis in human bone marrow stromal cells led to a transient, eightfold stimulation of Sox4, preceding the upregulation of *Sox5*, *Sox6* and *Sox9* mRNAs (Sekiya et al., 2002). Sox5, Sox6 and Sox9 regulate chondrocyte differentiation (Lefebvre et al., 1998), and Sox8 seems to regulate osteoblast differentiation through Runx2 inhibition (Schmidt et al., 2005).

In the present study we have examined the role of Sox4 in postnatal bone development in mice, with the hypothesis that the *Sox4* gene affects normal bone formation. Preliminary investigations indicated that healthy *Sox4*$^{+/-}$ mice developed osteopenia (Nissen-Meyer et al., 2004; Nissen-Meyer et al., 2005). Because ablation of both copies of the *Sox4* gene in mice leads to circulatory failure in utero (Schilham et al., 1996), we designed a longitudinal study of *Sox4*$^{+/-}$ mice and age- and gender-matched wild-type (WT) littermates, examining functional parameters of bone metabolism, histomorphometry, microcomputed tomography (μCT) and bone mineral densitometry related to age. To explore molecular and cellular mechanisms responsible for the observed osteopenia, we used primary cultures of differentiating *Sox4*$^{+/-}$ and WT calvarial osteoblasts to assess proliferation, differentiation and mineralization properties. In addition, we studied whether silencing of Sox4 in WT osteoblasts using small interfering RNA (siRNA) treatment could mimic the haploinsufficient phenotype of *Sox4*$^{+/-}$-derived osteoblasts. Our data indicate an important role for Sox4 in the regulation of bone formation and homeostasis.

Results

General morbidity of heterozygous *Sox4*$^{+/-}$ mice is low

Sox4$^{+/-}$ offspring was morphologically indistinguishable from WT, with an overall normal life span. However, rectal prolapses were more frequently observed in the *Sox4*$^{+/-}$ mice than in the WT; they also had somewhat reduced fertility. Internal organs and the skeleton were examined at time of sacrifice by an experienced pathologist (FPR) and apart from abdominal inclusion cysts in some females, no macroscopical differences were found between *Sox4*$^{+/-}$ and WT controls.

Sox4$^{+/-}$ mice were only slightly smaller than their littermates, as determined by total body mass (Table 1). Three-month-old *Sox4*$^{+/-}$ mice had significantly shorter femurs than WT (–4.6% for males, $P<0.001$; similar for females), whereas the differences were non-significant for older mice (not shown).

Table 1. Body mass, body fat and bone mineral density of WT and *Sox4*$^{+/-}$ mice

	Males		Females	
	WT (n=19)	*Sox4*$^{+/-}$ (n=11)	WT (n=18)	*Sox4*$^{+/-}$ (n=14)
Young mice (10 weeks)				
Body mass (g)	24.2±2.2	24.2±2.0	19.8±0.8	18.2±1.7^{B}
Body fat (%)	12.8±2.0	13.0±2.1	13.8±1.5	13.3±2.5
Bone area (cm^2)	8.65±0.59	8.78±0.30	8.35±0.39	8.08±0.45
BMD (mg/cm^2)				
Total body	46.47±2.42	44.40±2.18^{C}	43.89±1.19	40.57±2.13^{A}
Lumbar spine	67.11±4.62	61.17±3.43^{B}	62.81±4.52	57.69±5.29^{B}
Trochanter	80.87±7.52	76.80±5.79	73.79±4.86	67.61±6.39^{B}
Femoral shaft	61.01±7.69	60.15±5.08	50.55±4.13	48.81±2.84
Tibia^{D}	87.81±5.85	80.80±4.47^{C}	77.66±4.00	65.90±5.66^{B}
	WT (n=18)	*Sox4*$^{+/-}$ (n=8)	WT (n=20)	*Sox4*$^{+/-}$ (n=10)
Adult mice (6 months)				
Total mass (g)	31.2±2.7	29.5±2.5	24.6±2.7	23.6±2.4
Body fat (%)	17.0±5.7	19.1±3.4	19.1±4.6	22.3±3.4
Bone area (cm^2)	9.97±0.48	9.51±0.40^{C}	9.36±0.43	8.72±0.42^{A}
BMD (mg/cm^2)				
Total body	50.01±1.98	47.84±1.49^{C}	49.19±1.60	45.69±2.69^{A}
Lumbar spine	65.16±5.15	60.01±2.98^{C}	69.45±6.92	59.47±4.92^{A}
Trochanter	91.51±8.95	81.16±7.47^{B}	83.93±4.85	74.34±7.24^{A}
Femoral shaft	71.88±7.50	66.96±4.09	65.91±3.44	59.80±3.33^{A}
Tibia	98.18±7.05	90.51±6.66^{C}	93.63±4.50	84.70±9.13^{B}

Body mass, body fat, bone area and bone mineral density parameters were evaluated in vivo by repeated DXA measurements as described in the Materials and Methods and in the legend to Fig. 1A. The table shows the data from two observation points, young (10 weeks) and adult mice (6 months). Values represent mean ± s.d.

$^{A}P<0.001$; $^{B}P<0.01$; $^{C}P<0.05$ compared with gender-respective WT group using MANOVA; ^{D}Tibial bones were measured in smaller groups of 10-week-old mice; males: WT n=5, *Sox4*$^{+/-}$ n=6; females: WT n=7, *Sox4*$^{+/-}$ n=7.

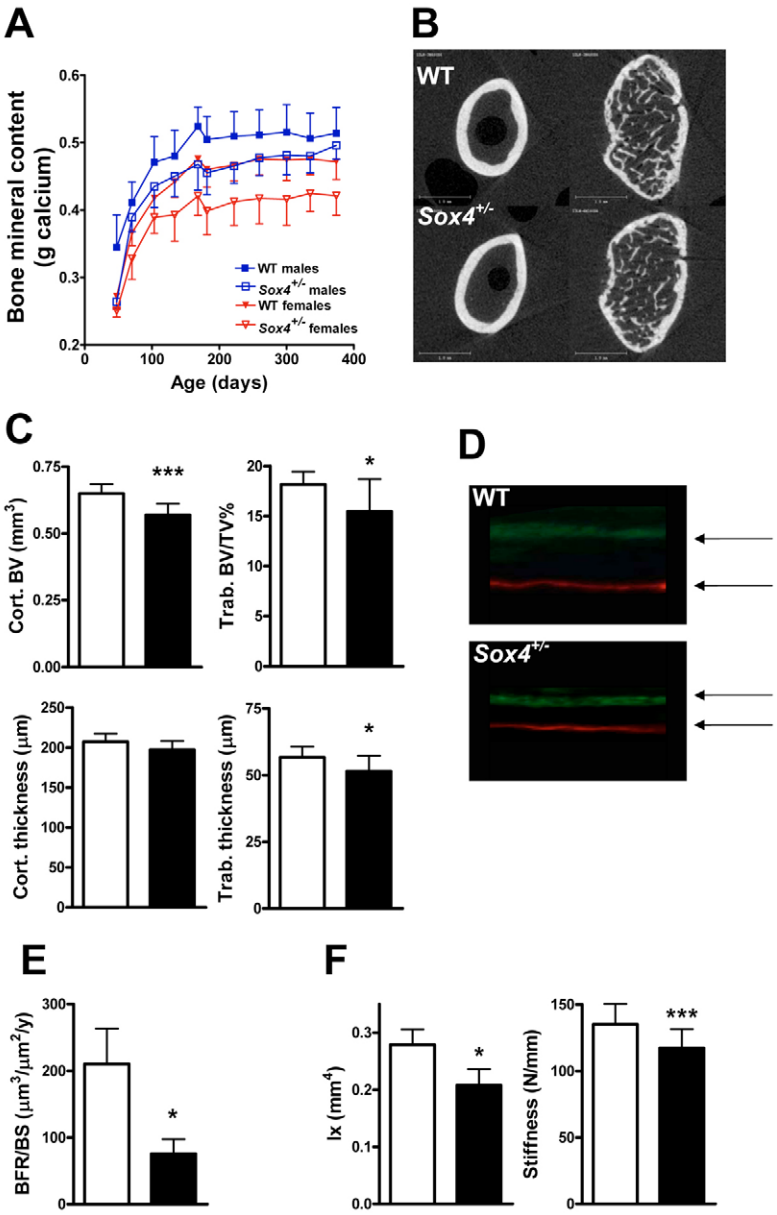

Fig. 1. Bone densitometric, morphological and biomechanical characteristics of *Sox4*$^{+/-}$ mice compared with WT. (A) BMC-changes with age measured with DXA in WT and *Sox4*$^{+/-}$ mice (n=11-24). Mean age for each measurement: 48, 70, 104, 134, 168, 182, 222, 260, 300, 335 and 374 days. The growth curves for each genotype in both genders (corrected for body weight and bone area) were significantly different (P<0.001) throughout the observation period. Plots of mean BMC ± s.d. (WT males and females: n=24; *Sox4*$^{+/-}$ males: n=11, *Sox4*$^{+/-}$ females: n=14). Error bars on one side were omitted for clarity. (B) Microarchitecture of diaphyseal and metaphyseal bone from WT and *Sox4*$^{+/-}$ mice analyzed by μCT. Typical example of femurs from 3-month-old males, left: diaphysis (cortical bone), right: methaphysis (trabecular bone). (C) Cortical bone volume (Cort. BV), cortical thickness, trabecular bone volume (Trab. BV/TV, %) and trabecular thickness in 3-month-old males. Bars, mean ± s.d. (WT: n=11, open bars; *Sox4*$^{+/-}$: n=8, solid bars). For cortical thickness, P=0.052. (D) Dynamic assessment of mineral acquisition rate (MAR) in WT and *Sox4*$^{+/-}$ mice. Fluoroscopic microphotograph showing fluorochrome labeling in a 3-month-old female injected with Alizarin (red) and calcein (green) 10 and 3 days before sacrifice, respectively. Distance between arrows: MAR during 7 days (see Table 3 for quantitative analysis). (E) Bone formation rate/bone surface/year (BFR/BS/year) in 3-month-old males treated as described in D. Bars, mean ± s.d. (WT: n=5, open bars; *Sox4*$^{+/-}$: n=4, solid bars). (F) Biomechanical properties: moment of inertia (Ix) and stiffness in femurs from 3-month-old males, presented as mean ± s.d. (WT: n=11, open bars; *Sox4*$^{+/-}$: n=8, solid bars). ***P<0.001; *P<0.05 compared with WT.

Bone mass in young *Sox4*$^{+/-}$ mice is reduced

We used repeated DXA (dual-energy X-ray absorptiometry) measurements to evaluate the age- and gender-related bone mineral content (BMC; Fig. 1A) and BMD (Table 1) in *Sox4*$^{+/-}$ and WT mice. From 7 weeks to 12 months of age, male and female *Sox4*$^{+/-}$ mice showed a significantly lower total bone area and whole body BMC and BMD (P<0.001 for all analyses of repeated measurements) compared with their WT littermates (Fig. 1A, Table 1). When specific regions of interest (ROI) were studied, *Sox4*$^{+/-}$ mice had significantly lower BMD compared with WT in both the axial (spine) and appendicular (trochanter femoris and tibia) skeleton (Table 1). Overall, the impact of *Sox4* haploinsufficiency on bone mass was manifest already by 10 weeks of age, and the differences remained throughout the observation period (corrected for bone area and body mass in both genders). There were no significant differences in body fat throughout the observation period (Table 1).

Impaired bone microarchitecture in *Sox4*$^{+/-}$ mice shown by μCT

Three-dimensional μCT analyses of femoral bones showed alterations of cortical and trabecular bone microarchitecture in *Sox4*$^{+/-}$ mice (Fig. 1B). By 3 months of age, cortical bone volume and cortical thickness at the femoral diaphysis were significantly lower in both male and female *Sox4*$^{+/-}$ mice compared with WT (Fig. 1C and Table 2). Moreover, male *Sox4*$^{+/-}$ mice showed significantly reduced total and medullary volume of cortical bone, indicating a decreased femoral bone size (diameter). These differences were maintained at 12 and 18 months of age (data not shown). At the distal femoral metaphysis, trabecular thickness was decreased and trabecular number slightly increased in 3-month-old *Sox4*$^{+/-}$ mice compared with WT (Fig. 1C and Table 2). Trabecular bone volume fraction (BV/TV) was decreased in males (Fig. 1C), whereas no differences in connectivity were seen between WT and *Sox4*$^{+/-}$ mice (Table 2). Altogether, the pattern of bone microarchitecture in heterozygous mice suggested a reduced bone formation during growth.

Static and dynamic bone histomorphometry in *Sox4*$^{+/-}$ mice

Data obtained by static histomorphometry of proximal tibiae from 3-month-old mice were similar to the μCT data from distal femur, showing lower values for trabecular BV/TV (%)

Table 2. Cortical and trabecular microarchitecture of femurs from WT and *Sox4*$^{+/-}$ mice by μCT analysis

	Males		Females	
	WT (*n*=11)	*Sox4*$^{+/-}$ (*n*=8)	WT (*n*=8)	*Sox4*$^{+/-}$ (*n*=7)
Cortical bone (diaphysis)				
Total volume (mm^3)	1.46±0.08	1.25±0.09^A	1.08±0.07	1.05±0.08
Bone volume (mm^3)	0.65±0.04	0.57±0.04^A	0.46±0.03	0.42±0.01^B
Cortical thickness (μm)	207.18±10.04	197.13±10.84^D	176.75±6.45	160.86±11.98^B
Medullary volume (mm^3)	0.81±0.08	0.68±0.06^A	0.62±0.05	0.62±0.09
Trabecular bone (distal femur metaphysis)				
BV/TV (%)	18.16±1.29	15.46±3.24^C	4.54±0.51	4.83±1.01
Trabecular number (/mm)	4.71±0.27	5.14±0.17^A	3.68±0.34	4.19±0.27^B
Trabecular thickness (μm)	56.66±4.01	51.48±5.83^C	38.50±3.01	33.56±1.50^B
Trabecular connectivity (mm^{-3})	117.42±18.60	118.61±18.85	21.38±5.59	29.08±24.21

Three-dimensional microarchitectural parameters were evaluated ex vivo on excised bones from 3-month-old mice. Values represent mean ± s.d. $^A P<0.001$; $^B P<0.01$; $^C P<0.05$, $^D P=0.052$ compared with gender-respective WT group using MANOVA.

and thickness in *Sox4*$^{+/-}$ mice versus WT (data not shown). Osteoid volume/bone volume, osteoblast surface/bone surface (BS) and growth plate width were all significantly lower in tibiae from *Sox4*$^{+/-}$ mice versus WT (Table 3). The zone of hypertrophic chondrocytes and the osteoclast surface:BS ratio were not significantly changed, but for both there was a trend towards reduction (Table 3). At 6 months of age, histomorphometric analyses of tibial bones from both genders corresponded to μCT data at this age, showing no significant differences between the WT and *Sox4*$^{+/-}$ mice for the parameters mentioned (not shown).

Dynamic double fluorochrome labeling (using calcein and Alizarin Red) of bone accretion showed a marked (>50%) reduction of mineral apposition rate (MAR) in 3-month-old *Sox4*$^{+/-}$ compared with WT mice (Fig. 1D, Table 3), consistent with the reductions in bone formation rate (BFR; Fig. 1E) and mineralized surface/BS (Table 3). Taken together, these results suggested that reduced bone mass in *Sox4*$^{+/-}$ mice was because of a defect in bone formation rather than in bone resorption.

Deteriorated bone strength in *Sox4*$^{+/-}$ mice

To evaluate the influence of *Sox4* haploinsufficiency on cortical bone mechanical properties, the area moment of inertia (Ix) was derived from the geometrical measurements obtained by μCT, and the structural (ultimate force and stiffness) and material (Young's elastic modulus and ultimate stress) properties related to fracture resistance were directly evaluated by three-point bending of femurs. As shown in Table 4 and Fig. 1F, Ix, ultimate force and stiffness of femurs were significantly lower in male and female *Sox4*$^{+/-}$ compared with WT mice. However, Young's elastic modulus and ultimate stress were similar in male and female *Sox4*$^{+/-}$ and WT mice, indicating that the decreased bone strength in *Sox4*$^{+/-}$ mice was due primarily to the smaller diameter of their diaphyseal bone.

Bone formation markers and PTH/calcium status in serum from *Sox4*$^{+/-}$ mice

The serum levels of the bone formation marker osteocalcin (OCN) were moderately reduced in 3-month-old female *Sox4*$^{+/-}$ mice (165.3±24.0 ng/ml; mean ± s.d.) compared with WT (182.1±49.8 ng/ml; *n*=5 in both groups), but alkaline phosphatase (ALP) activity was not (132.9±9.6 mU/ml serum in *Sox4*$^{+/-}$ versus 114.8±6.5 mU/ml serum in WT; $P<0.01$; *n*=5 and 7, respectively). Serum levels of PTH and total calcium measured at 6 and 12 months were similar in the WT and *Sox4*$^{+/-}$ mice (data not shown).

Sox4$^{+/-}$ osteoblasts in primary cultures show serious functional defects

The effect of Sox4 on osteoblast development and function was

Table 3. Histomorphometric analysis in WT and *Sox4*$^{+/-}$ mice

	Males		Females	
	WT (*n*=5)	*Sox4*$^{+/-}$ (*n*=4)	WT (*n*=4)	*Sox4*$^{+/-}$ (*n*=3)
Static parameters				
Growth plate width (μm)	105.75±7.55	84.02±2.06^B	103.87±6.92	87.70±1.81^B
Hypertrophic chondrocyte zone (μm)	40.91±1.38	39.14±1.85	45.37±4.97	34.98±7.89
Osteoid volume/bone volume (%)	2.69±0.17	1.85±0.13^A	2.20±0.21	1.59±0.19^B
Osteoblast surface/bone surface (%)	15.89±0.60	10.86±2.60^B	32.90±6.64	20.26±4.50^B
Osteoclast surface/bone surface (%)	10.25±4.99	8.14±3.25	9.26±1.62	7.65±1.10
Dynamic parameters				
Mineral apposition rate (μm/day)	1.41±0.40	0.67±0.15^B	1.49±0.39	0.63±0.39^B
Bone formation rate/bone surface (μm^3/μm^2/year)	210.57±52.95	75.93±21.60^B	258.68±72.78	94.12±16.57^B
Mineralizing surface/bone surface (%)	41.06±6.18	27.76±1.95^B	47.32±3.80	32.21±4.53^B

Parameters from trabecular bone (proximal tibia metaphysis), analysed 100 μm from distal end of growth plate excluding the endocortical surfaces (3-month-old mice). Values represent mean ± s.d.
$^A P<0.01$; $^B P<0.05$ compared with WT of same gender (Student's *t*-test).

Table 4. Femur bone geometry and strength in WT and *Sox4*$^{+/-}$ mice

	Males		Females	
	WT (*n*=11)	*Sox4*$^{+/-}$ (*n*=8)	WT (*n*=7)	*Sox4*$^{+/-}$ (*n*=8)
Moment of inertia, Ix (mm^4)	0.279±0.026	0.208±0.029^C	0.149±0.021	0.136±0.014
Ultimate force (N)	20.4±1.4	16.7±1.6^C	12.8±1.7	10.8±1.1^A
Stiffness (N/mm)	135.2±15.2	117.3±14.1^A	93.3±16.0	79.8±10.6
Young's elastic modulus, E (MPa)	3506±647	4089±732	4469±435	4221±676
Ultimate stress (GPa)	108.6±10.2	110.3±8.4	109.9±9.3	100.0±10.8

Values are mean ± s.d. as derived from μCT (Ix) and evaluated by three-point bending of femurs from 3-month-old mice. $^A P<0.001$; $^B P<0.01$; $^C P<0.05$ compared with gender-respective WT group using MANOVA.

evaluated in primary calvarial cell cultures derived from *Sox4*$^{+/-}$ and WT mice. Real-time PCR analysis showed 42% reduction in levels of *Sox4* mRNA in *Sox4*$^{+/-}$ osteoblasts versus WT (Fig. 2A). By comparison, bone tissue from 3-month-old male *Sox4*$^{+/-}$ mice also expressed lower levels of *Sox4* mRNA (69%; P=0.056) relative to age- and gender-matched WT mice. Similarly, the mRNA levels for *Osx*, *OCN*, *collagen type I A2* (*Coll1A2*) and *ALP* were significantly lower in the *Sox4*$^{+/-}$ osteoblast cultures (P<0.05), whereas *Runx2*, *BMP-2*, *osteopontin* (*OPN*), *PTH/PTHrP-receptor-1* (*PTHR1*), *PTH-related peptide* (*PTHrP*) and *c-fos* were unchanged (Fig. 2A). Osteoclast-regulating cytokines produced by primary osteoblast cultures were largely unaffected (Table 5), as was production of the adipocyte markers PPARγ and AP-2, and the estrogen receptor ERα (data not shown). A corresponding decline in Sox4 protein levels was observed in *Sox4*$^{+/-}$ osteoblasts relative to WT, as assessed by western blot analysis (Fig. 2B), whereas ALP activity and the number of mineralized bone nodules (by von

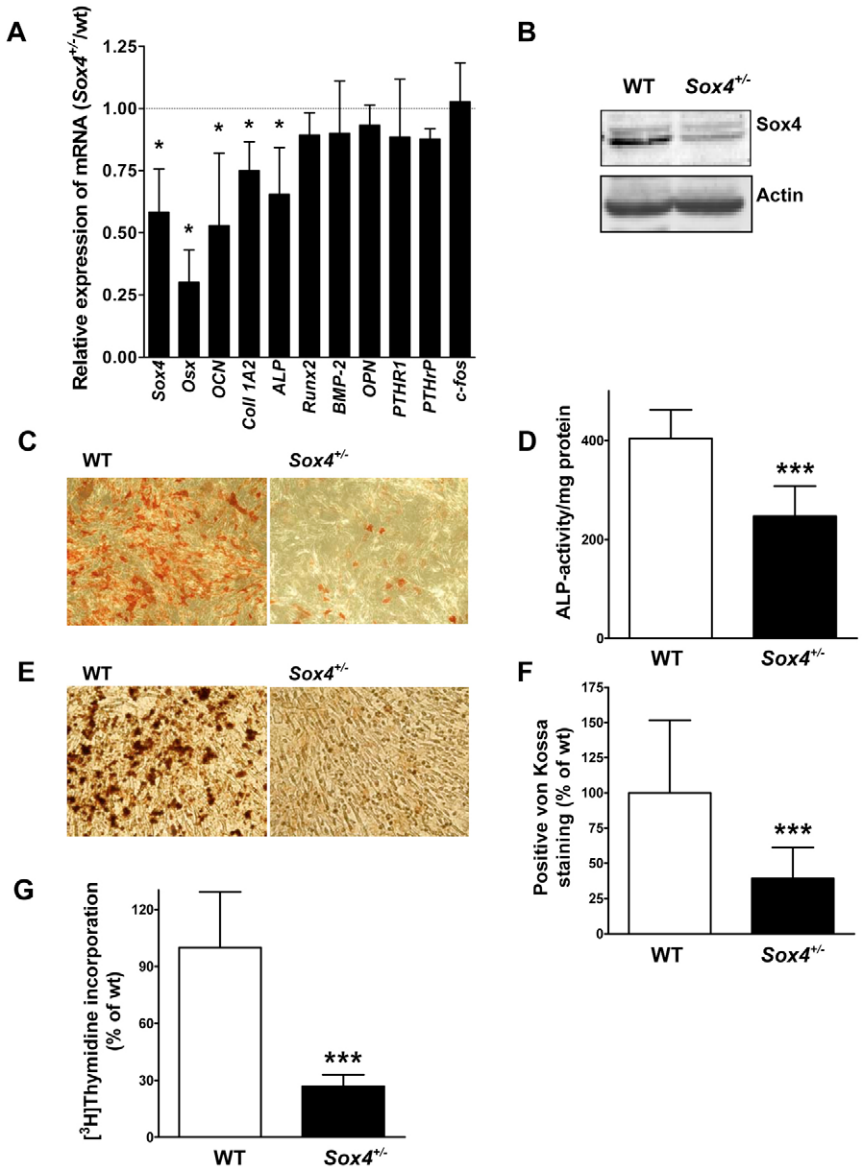

Fig. 2. Primary cultures of calvarial osteoblasts derived from *Sox4*$^{+/-}$ and WT mice. (A) Real-time PCR analyses of osteoblast characteristic mRNAs extracted from *Sox4*$^{+/-}$ and WT primary osteoblast cultures: *Osx*, osterix; *OCN*, osteocalcin; *Coll1A2*, collagen1A2; *ALP*, alkaline phosphatase; *Runx2*; *BMP-2*, bone morphogenetic protein-2; *OPN*, osteopontin; *PTHR1*, PTH/PTHrP-receptor-1; *PTHrP*, PTH-related peptide. Results (from three independent experiments) were normalized to *β-actin* or *GAPDH*, and expression in *Sox4*$^{+/-}$ cells is presented relative to WT (set to 1, broken line). (B) Representative immunoblot of lysates from WT and *Sox4*$^{+/-}$ osteoblasts, using anti-Sox4 and anti-actin antibodies as described in the Materials and Methods. (C) Representative micrographs of ALP histochemical staining (20× magnification) in WT and *Sox4*$^{+/-}$ osteoblasts cultured for 7 days (n=4). (D) Biochemical quantification of ALP activity in the osteoblast cultures shown in C. (E) Micrographs of von Kossa-stained osteoblast cultures (20× magnification) demonstrating mineralization (dark areas) of nodules after 3 weeks of culture in medium containing ascorbic acid and β-glycerophosphate. (F) Densitometric quantification of von Kossa-stained mineralized nodules expressed as per cent of WT staining. In each of three independent experiments, 4-10 representative microscopic fields were examined. (G) Incorporation of [^{3}H]thymidine in proliferating osteoblasts. Data from two independent experiments were normalized and compared with mean WT values (n=24 for each genotype). Bars, mean ± s.d. ***P<0.001, *P<0.05, unpaired Student's t-test (with Welch correction in F).

Table 5. Osteoclast-regulating cytokines produced by primary osteoblast cultures from WT and *Sox4*$^{+/-}$ mice

	Sox4$^{+/-}$/WT ratio (*n*=3)
IL-1β	1.29±0.29
IL-6	0.77±0.2
M-CSF	0.99±0.08
PTHrP	1.16±0.16
TNFα	1.11±0.34
RANKL	0.76±0.24
OPG	0.90±0.25
IL-12	1.18±0.43
IL-18	0.93±0.23
GM-CSF	1.40±0.49

mRNAs of osteoclast-regulating cytokines characteristically produced by primary osteoblasts in culture, quantified by real-time RT-PCR and reported as mean expression (± s.d.) in *Sox4*$^{+/-}$ osteoblast cultures relative to WT (set equal to 1; *n*=3, each time performed in triplicate). Student's *t*-tests revealed no significant differences between WT and *Sox4*$^{+/-}$ cultures.

Kossa staining) were reduced by approximately 40 and 60%, respectively (Fig. 2C-F). The total cell number in *Sox4*$^{+/-}$ calvarial cultures was markedly lower compared with WT (52±13 and 88±23, $P<0.01$; $n=3$). However, the relative fraction of ALP-positive cells was even further reduced (50±13% and 81±8% in *Sox4*$^{+/-}$ and WT osteoblasts, respectively; $P<0.001$). Moreover, we assessed the proliferative capacity of *Sox4*$^{+/-}$ osteoblasts by thymidine incorporation, and found that it was severely impaired, being only 27% relative to WT (Fig. 2G). Taken together, these data demonstrate *Sox4*$^{+/-}$ osteoblast insufficiency in vitro.

No functional defects detected in bone marrow-derived primary cultures of *Sox4*$^{+/-}$ osteoclasts

No differences in typical osteoclastogenic properties were detected, as judged by the number of tartrate-resistant acid phosphatase (TRAcP)-positive multinucleated cells (96±33% in *Sox4*$^{+/-}$ cells versus WT; $n=4$) and the ability to erode bone in vitro, shown as functional pit index assay (119±35.2% in *Sox4*$^{+/-}$ cells versus WT; $n=4$). WT osteoclastic cells cultured in the presence of conditioned cell media from *Sox4*$^{+/-}$ osteoblasts showed unchanged light microscopic morphology, phenotype and functional activity (not shown).

Sox4 siRNA modulates WT osteoblast function, mimicking *Sox4* haploinsufficiency

To study the effect of knockdown of *Sox4*, we treated primary calvarial osteoblasts from WT mice with siRNA against *Sox4* or with scrambled siRNA as control. Real-time PCR demonstrated a decline in levels of *Sox4* mRNA by 63% relative to control cells (Fig. 3A). Significant reductions in mRNA levels were found also for *Osx*, *OCN*, *Coll1A2*, *PTHR1*, *PTHrP* (29-52%) and *ALP* (75%), whereas *Runx2* and *OPN* were not affected (Fig. 3A). Cell proliferation analysis replicated previous results in *Sox4*$^{+/-}$ osteoblasts: Sox4 siRNA reduced [^{3}H]thymidine incorporation by 54% compared with WT (Fig. 3B). Furthermore, the number of cells staining positive for ALP was reduced by 31% and ALP enzymatic activity by 33% (Fig. 3C-E). Similar to the *Sox4*$^{+/-}$ osteoblast cultures described above, Sox4 siRNA treatment caused lower cell numbers (41±1.5 versus 61±6.3), and relative reductions in the number of ALP-positive cells (44±7% in Sox4 siRNA-treated cultures versus 64±14% in the control cultures, $P<0.05$). We did not find evidence

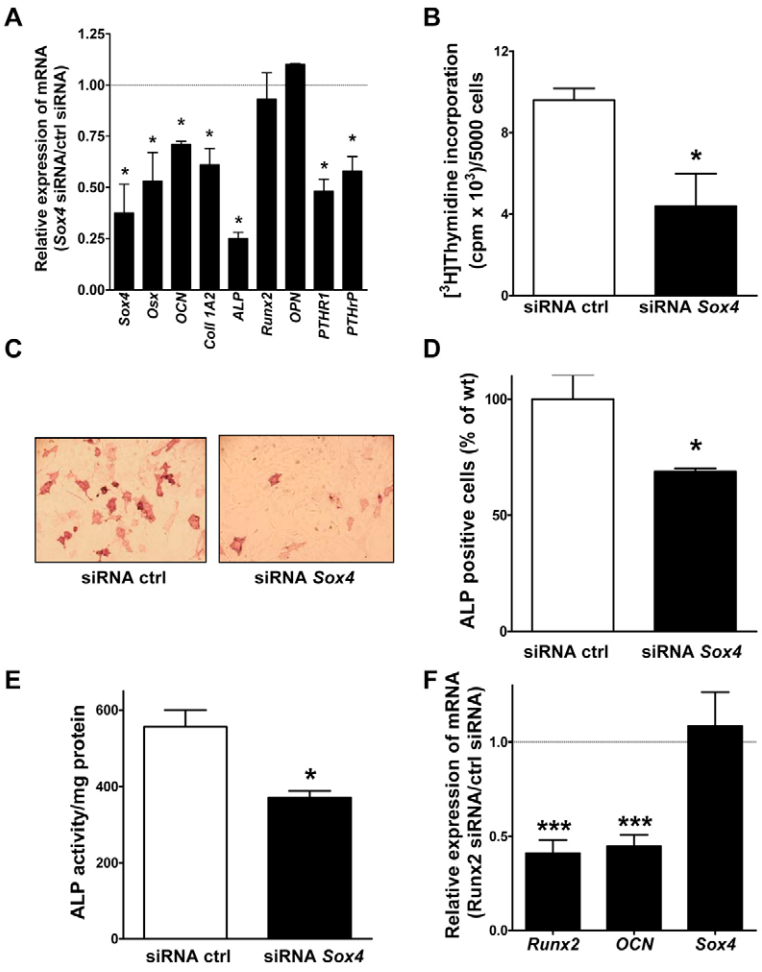

Fig. 3. Silencing of *Sox4* mRNA in WT primary osteoblast cultures with siRNA. (A) Real-time RT-PCR analyses of mRNA levels in siRNA-treated osteoblasts expressed relative to osteoblasts treated with control (scrambled) siRNA (set to 1, broken line), and normalized to *GAPDH* mRNA. *Osx*, osterix; *OCN*, osteocalcin; *Coll1A2*, collagen1A2; *ALP*, alkaline phosphatase; *Runx2*; *OPN*, osteopontin; *PTHR1*, PTH/PTHrP-receptor-1; *PTHrP*, PTH-related peptide. (B) Incorporation of [^{3}H]thymidine in proliferating WT osteoblasts following treatment with control or Sox4 siRNA, respectively. (C) Photomicrographs of WT osteoblast cultures treated with control or Sox4 siRNA, respectively, stained for ALP activity. (D) Quantification of ALP-positive cells per well in C. (E) Biochemical activity of ALP in siRNA-treated osteoblasts. (F) mRNA levels of *Runx2*, *OCN* and *Sox4* following treatment of WT cells with specific Runx2 siRNA compared with control siRNA, quantified by real-time RT-PCR and related to *GAPDH* mRNA as control (set to 1, broken line). In A,B,D-F: ***$P<0.001$, *$P<0.05$ versus siRNA control (ctrl); bars, mean ± s.d. of triplicates ($n=2$).

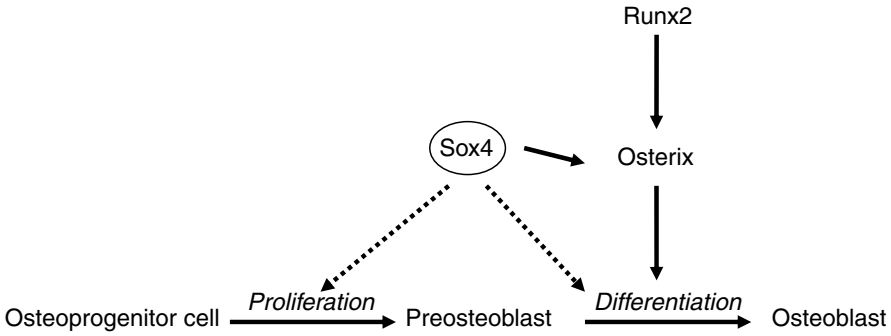

Fig. 4. Proposed model of Sox4 regulation of osteoblast proliferation and differentiation. Represented is the hierarchy of the osteoblast lineage and the predicted Sox4 actions. According to the experimental data, Sox4 could affect proliferation of osteoprogenitors as well as differentiation of mature osteoblasts. This latter action could be exerted by downregulation of osterix, with a mechanism apparently independent of Runx2.

that treatment of osteoblasts with Sox4 siRNA induced apoptosis (data not shown).

Runx2 siRNA modulates osteoblast differentiation without affecting *Sox4* expression

Our data showing reduced expression of two typical Runx2-dependent genes, *Osx* and *OCN*, both in *Sox4*$^{+/-}$ and Sox4 siRNA-treated osteoblasts, might suggest that Sox4 and Runx2 are part of the same molecular pathway involved in regulating osteoblast development and/or function. Thus, gene silencing of *Runx2* by siRNA technology was used to assess whether Sox4 is affected by decreased Runx2 levels in mouse primary calvarial osteoblasts. We found no effect of *Runx2* knockdown on *Sox4* mRNA expression, whereas *Runx2* and *OCN* mRNA levels were downregulated by 65% and 62%, respectively (Fig. 3F). These results suggest that Sox4 action on osteoblastogenesis is independent of the Runx2 pathway (Fig. 4).

Discussion

Sox4 belongs to a family of HMG box transcription factors regulating numerous developmental processes. In this study we have characterized the skeletal phenotype of *Sox4*$^{+/-}$ mice and the functional role of Sox4 in osteoblasts. Our results establish that Sox4 is important for normal postnatal bone development, through effects on osteoblast development or function.

Even though *Sox4*$^{+/-}$ mice thrived and exhibited normal gross anatomy from birth, bone mass indices were significantly reduced (compared with WT littermates) already by 7-10 weeks of age. Histomorphological analyses showed reduced thickness of cortical and trabecular bone, in addition to markedly lower (>50%) BFR and MAR, in 3-month-old *Sox4*$^{+/-}$ mice versus WT. Importantly, biomechanical bone strength (fracture resistance) in femur was also affected, most likely because of a smaller diaphyseal diameter. In light of the striking reductions in MAR and other histomorphometric parameters (Table 3), we cannot exclude the possibility that the relatively modest quantitative effects of *Sox4* haploinsufficiency on bone mass parameters in vivo may involve compensatory mechanisms. However, dynamic parameters for bone formation velocity at a given time (MAR, BFR) are not directly comparable to BMC, which integrates net mineralized bone tissue formed over the lifetime of the animal. Nevertheless, our results clearly demonstrate that *Sox4*$^{+/-}$ mice exhibit an osteopenic phenotype, including impaired bone structure and biomechanical strength, mainly caused by suppressed bone formation and/or mineralization in early life.

The differences between *Sox4*$^{+/-}$ and WT mice appear most pronounced at 3 months of age; in addition to bone mass, the differences in femoral length and bone structure (by μCT and static histomorphometry) peaked at 3 months and lost significance in older age. Moreover, our histomorphometry data showing reduced osteoid volume in bones from *Sox4*$^{+/-}$ mice do not support a mineralization defect (e.g. osteomalacia) as a major responsible factor for the observed low bone mass. These findings strongly indicate that Sox4 is a limiting factor for normal bone development during periods of active and intense growth. Following peak bone mass and skeletal maturation, the osteopenia did not worsen but was maintained in both genders during adult life, suggesting that in later stages of adulthood, reduced levels of Sox4 are sufficient to sustain normal bone homeostasis. Importantly, our results also indicate that the bone phenotype in *Sox4*$^{+/-}$ mice cannot be fully rescued by other members of the Sox family.

The suboptimal skeletal development and osteopenic phenotype in *Sox4*$^{+/-}$ mice are interesting in relation to genetic factors regulating early stages of bone formation. We have previously shown that *Sox4* mRNA is highly expressed in hypertrophic chondrocytes of the mouse embryonic growth plate during early phases (ED15.5) of endochondral bone development, and also by human and rodent osteoblasts in vitro (Reppe et al., 2000). Whereas cRNA in situ hybridization was not sufficiently sensitive to detect *Sox4* mRNA in osteoblasts in vivo, real-time PCR enabled us to verify reduced *Sox4* expression in bones from *Sox4*$^{+/-}$ mice relative to WT (in vivo), as well as in the respective calvarial osteoblast cultures derived from these animals (in vitro).

Another group has reported that highest levels of *SOX4* mRNA expression were seen in the proliferative phase during the course of human osteoblast development (Billiard et al., 2003). In the present study we found severely impaired proliferation of *Sox4*$^{+/-}$ osteoblasts, as assessed by a decreased thymidine incorporation rate of 73%, and reduced numbers of cells. In support of these observations, preliminary cell-cycle analyses indicated delayed S-phase progression and slower passage into the G2 phase in *Sox4*$^{+/-}$ osteoblasts (data not shown), suggesting that it takes mutant cells longer to traverse the cell cycle. Delayed osteoblast maturation was also demonstrated in *Sox4*$^{+/-}$ calvarial cultures, with *Osx*, *OCN*, *Coll1A2* and *ALP* mRNA levels selectively reduced (25-70%), whereas the other mRNAs investigated were not changed. These changes in the osteoblast gene expression pattern in *Sox4*$^{+/-}$ cells were almost entirely mimicked by siRNA treatment of WT osteoblasts (with the exception of *PTHR1* and *PTHrP*, see below). By contrast, no significant effect of the

Sox4 mutation was observed on osteoclast development and function in vitro. Hence, our data support a predominant effect of Sox4 deficiency on bone formation, and implicate this transcription factor as an important regulator of osteoblast proliferation. Whether the delay in osteoblast maturation, at least partly, is secondary to the defect in proliferation remains to be established.

The localization of *SOX4* to chromosome 6p22 (in humans) and 13 (in mice) (Critcher et al., 1998) coincides with a mapped chromosomal region recently predicted to comprise a gene with pleiotropic effects on osteoblast activity, number or recruitment in baboons (Havill et al., 2006) and to affect BMD in mice (Shimizu et al., 2002). In light of our data in the present study, it will be important (in future research) to clarify whether this gene is identical to *Sox4*. The upregulation of human *SOX4* mRNA in patients with primary hyperparathyroidism (Reppe et al., 2006), together with our results that *SOX4* is downregulated in postmenopausal primary osteoporosis (K.M.G., S.R., V.T.G., R.J., F.P.R., L.S.H.N.-M. and O. K. Olstad, unpublished), strengthen the concept that SOX4 has a functional role in human bone metabolism.

Acute *Sox4* knockdown (>50% by siRNA) in normal calvarial osteoblasts in vitro reduced the mRNA levels for *PTHR1* and *PTHrP*, which is interesting also in light of our previous observation that *Sox4* is a PTH-responsive gene (Reppe et al., 2000). Thus, Sox4 is not only a target for PTHR1 signaling, but may also be part of a regulatory loop that modulates the PTH/PTHrP-receptor system (Kronenberg, 2006). This effect of *Sox4* gene silencing on *PTHR1* and *PTHrP* mRNAs was clearly distinct from the pattern found in $Sox4^{+/-}$ osteoblasts, and the reason for the apparent discrepancy between long-term versus acute effects of Sox4 deficiency remains to be clarified.

The transcription factors Runx2 and Osx play crucial roles in osteoblastogenesis, as indicated by severe defects in bone development following knockout of these genes (Komori et al., 1997; Nakashima et al., 2002). Runx2, an important regulator of the osteoblast-related protein OCN (Ducy, 2000; Gaur et al., 2005), also modulates *ALP* and *Osx* expression, whereas Osx is not required for expression of Runx2 (Nakashima et al., 2002). Thus, Osx acts downstream of Runx2 to regulate osteoblast differentiation (Nakashima et al., 2002), but also mediates other signaling pathways including BMP-2 and IGF-1 (Celil et al., 2005), independent of Runx2. Our results from Sox4 siRNA experiments are in agreement with a Runx2-independent mechanism for Sox4 action in osteoblast development. Whereas mRNA for *Osx* was markedly decreased in Sox4 siRNA-treated WT osteoblasts, as well as in $Sox4^{+/-}$ osteoblast cultures, *Runx2* was not affected. Furthermore, treatment of WT osteoblasts with Runx2 siRNA did not reduce *Sox4* expression. It is possible that the effect of Sox4 on osteoblast development, as assessed by mRNAs for *ALP* and *OCN*, is mediated by Osx, but independent of Runx2 (Fig. 4). Analysis of the promoter sequences of *OCN* (data not shown) and *Osx* (Lu et al., 2006) revealed several putative binding sites for Sox-like transcription factors in these genes; therefore, direct transcriptional regulation through Sox4 cannot be excluded.

Growth plate width was significantly reduced in limbs from $Sox4^{+/-}$ mice, suggesting that chondrocytes are also affected by Sox4 deficiency (Table 3). Because there was no evidence for alterations in the number or activity of osteoclasts/chondroclasts in bones from $Sox4^{+/-}$ mice, the primary responsible mechanism for reduced growth plate width is most likely related to reduced ability of columnar chondrocytes to proliferate and subsequently undergo hypertrophy (Vanky et al., 1998). The zone of hypertrophic chondrocytes was slightly diminished, although not significantly, in the same limbs (Table 3). It is also noteworthy that (activated) PTH/PTHrP receptors delay chondrocyte hypertrophy through both Runx2-dependent and -independent pathways (Guo et al., 2006). Whether reduction in growth plate width in $Sox4^{+/-}$ mice relative to WT is associated with disturbances in PTHR1-mediated signaling in chondrocytes, and the potential involvement of Runx2 (through dependent and independent pathways) in this process, are interesting topics that need to be addressed in further studies.

In conclusion, we have characterized the skeletal phenotype of *Sox4* haploinsufficient mice and investigated the functional role of Sox4 deficiency in osteoblastogenesis in vitro. Our results demonstrate that Sox4 influences bone formation both in vivo and in vitro, by modulating osteoblast maturation and function. These results implicate Sox4 as an important regulator of osteoblast proliferation and differentiation, and suggest that Sox4 action is mediated at least partly by Osx, but is independent of Runx2. Finally, we find that Sox4 deficiency results in reduced growth plate width, with the capacity to modulate skeletal growth.

Materials and Methods

Animal breeding

$Sox4^{+/-}$ heterozygous mice from a C57Bl/6 background were a gift from Hans Clevers (Hubrecht Laboratory, Netherlands Institute for Developmental Biology, Utrecht, The Netherlands) (Schilham et al., 1996), and all mice used in the present study have been backcrossed in the same strain for >10 consecutive generations. The animals were kept and bred in local animal facilities in Oslo, Norway and L'Aquila, Italy, following FELASA guidelines, and all animal procedures were approved by the committees for animal research in Norway and Italy. Pups were separated and earmarked at 3 weeks of age, and the resulting earpieces were used for genotyping using a DNeasy tissue purification kit (Qiagen) and PCR with two sets of specific primers: NEO749 (forward) 5′-ACAAGATGGATTGCACGCAGG-3′, NEO1119 (reverse) 5′-GAATGGGCAGGTAGCCGGATC-3′; Neo-f1 (forward) 5′-AGGATCTCCTGTCATCTCACCTTGCTCCTG-3′ and Neo-rev1 (reverse) 5′-AAGAACTCGTCAAGAAGGCGATAGAAGGCG-3′ (Invitrogen). Before preparation of osteoblast and osteoclast cultures (postnatal day 8-10), genotyping was performed on earpieces obtained at day 6-8.

BMD and BMC measurements

$Sox4^{+/-}$ mice and WT littermates were at regular time intervals anaesthetized with subcutaneous (s.c.) injections of Hypnorm (Cilag) and Dormicum (Roche; 0.05-0.075 ml/kg, working solution: 1.25 mg/ml midazolam, 2.5 mg/kg fluanisone and 0.079 mg/kg fentanyl citrate), and subjected to BMD/BMC measurements by DXA in a PIXImus densitometer (GE Medical systems/Lunar Corp.). Calibrations were performed with a phantom mouse with a defined value, and quality assessments were performed before each use. The coefficient of variation for total BMD is 0.59%.

ROIs were analyzed using the PIXImus software (v1.46) and include total body (the calvarium, mandible and teeth were excluded), three lumbar vertebrae (ca 17×55-59 pixels), trochanter femoris, femoral midshaft and proximal tibia of right hindlimb (all 17×11 pixels). Age- and sex-matched groups of mice were measured repeatedly at ~6-week intervals for 12 months, starting at 7-10 weeks. Measurements were performed twice with animal repositioning between scans, and mean values were analyzed using Microsoft Excel. Repeated measurements (ex vivo) of identical bone areas with repositioning gave a coefficient of variation of ±1.4%.

Dynamic and static histomorphometry

10-week-old $Sox4^{+/-}$ and WT mice were injected subcutaneously with Alizarin Complexone (Sigma; 20 mg/kg body weight) and calcein (Fluka; 30 mg/kg body weight) 10 and 3 days before sacrifice, respectively (Marzia et al., 2000). Both tibiae were dissected and fixed in 4% formaldehyde followed by embedding in a methyl

methacrylate resin (Technovit 9100 New; Heraeus Kulzer GmbH, Wehrheim, Germany) for dynamic histomorphometry. The following parameters were calculated: MAR (μm/day), BFR/BS ($\mu m^3/\mu m^2$/year) and mineralizing surface (MS/BS, %).

Histomorphometric measurements were performed as previously described (De Benedetti et al., 2006; Marzia et al., 2000) and with the suggested nomenclature (Parfitt et al., 1987). Briefly, one tibia from each animal was sectioned longitudinally through the frontal plane. Undecalcified sections (~2 μm-thick) were stained with Methylene blue/azure II for quantitative analysis of structural variables of trabecular metaphyseal bone, and osteoblasts. Osteoclasts were evaluated in adjacent sections treated for the cytochemical demonstration of TRAcP. The following variables were measured in the proximal tibia: (1) trabecular bone volume/tissue volume (BV/TV, %); (2) trabecular thickness (μm), trabecular number (no./mm) and trabecular separation (μm), derived according to the parallel plate model (Parfitt et al., 1983) and measured in the same zone as BV/TV; (3) growth plate width (μm) and size of the hypertrophic chondrocyte zone (μm); (4) osteoid volume (OV/BV, %) and osteoblast surface (%); (5) osteoclast surface (%). Osteoid volume, osteoblasts and osteoclasts were measured in a metaphyseal region extending at least 100 μm away from the distal end of the growth plate and excluding the endocortical surfaces.

μCT scanning

We assessed trabecular and cortical bone architecture using μCT (μCT40; Scanco Medical AG, Basserdorf, Switzerland), employing a 12-μm isotropic voxel size. Specifically, trabecular bone architecture was evaluated at the distal femoral metaphysis, whereas cortical bone morphology was evaluated at the femoral mid-shaft, as previously described (Bouxsein et al., 2005; Ferrari et al., 2005). Bones from mice aged 3, 6, 12 and 18 months were examined.

For all μCT evaluations, we used a nominal isotropic voxel size of 12 μm. Morphometric parameters, including BV/TV (%), trabecular number (mm^{-1}), trabecular thickness (μm), trabecular separation (μm), structure model index (SMI) and connectivity density (mm^{-3}), were computed without assumptions regarding the underlying bone architecture (Hildebrand and Ruegsegger, 1997). At the femoral midshaft, 50 transverse CT slices were obtained and used to compute the total volume within the periosteal envelope (mm^3), cortical bone volume (BV, mm^3), medullary volume (mm^3) and cortical thickness (μm). We also used the CT images to measure the bone inner and outer diameter (r_i and r_o, mm). The femurs were approximated as perfect tubes and the area moments of inertia (I_x, mm^4) at the midshaft approximated by $I_x=\pi(r_o^4-r_i^4)/4$.

Femur biomechanical testing

Bones from 3-month-old mice were rehydrated at room temperature in phosphate-buffered saline (PBS) and femoral biomechanical properties were assessed by three-point bending (Brodt et al., 1999; Jepsen et al., 2003), using the Instron Microtester 5848 (Instron, Norwood, MA) equipped with a 100-N gauge and custom bone supports with a 7-mm distance. Load was applied at a constant rate (0.02 mm/sec) until failure and the force-displacement data sampling was set to 100 Hz. We measured the ultimate force (N) and bending stiffness (N/mm) from the load-displacement curve and computed the Young's elastic modulus, E (GPa), and ultimate stress (MPa) using the relevant mid-femoral cross-sectional geometry measured from μCT and following the method described by Schriefer et al. (Schriefer et al., 2005).

Serum analyses

Serum was collected from WT and *Sox4*$^{+/-}$ mice sacrificed at the same time of the day to avoid diurnal fluctuations of serum markers. Measurements of total serum calcium and PTH were performed using the QuantiChrom Calcium Assay Kit (DICA-500; BioAssay Systems, Hayward, CA) and the Mouse Intact PTH ELISA Kit (Immunotopics, San Clemente, CA), following the respective protocols. Serum OCN was measured using the Mouse Bone Panel 1B Lincoplex kit (Cat# MBN1B-41K) following the manufacturer's protocol (LINCO Research, St Charles, MO), and analyzed with a BioPlex luminometer (Bio-Rad Laboratories). ALP activity was measured as described (Dimai et al., 1998).

Primary cultures of mouse calvarial osteoblasts

Osteoblast cultures were derived from 8-day- to 10-day-old *Sox4*$^{+/-}$ and WT mice of both genders as described (Marzia et al., 2000). Initial experiments using separate osteoblasts from male and female mice showed similar results for all functional parameters tested. We therefore used gender-mixed osteoblast cultures for most experiments. Briefly, dissected calvariae were sequentially digested with 1 mg/ml Clostridium histiolyticum type IV collagenase (Sigma) and 0.025% trypsin (Becton Dickinson) in Hank's buffered solution. Cells from second and third digestions were grown in Dulbecco's modified Eagle's medium (DMEM) with antibiotics and 10% fetal bovine serum (FBS). At confluence, cells were trypsinized, counted and plated in appropriate vessels for further experiments. All experiments were performed on 7-day cultures or as indicated. Cell culture media and supplements were purchased from Invitrogen (Carlsbad, CA).

Western blotting

Cells were lysed in RIPA buffer (50 mM Tris HCl, pH 7.5, 150 mM NaCl, 1% Nonidet P-40, 0.5% sodium deoxycholate, 0.1% SDS) containing protease inhibitors. 100 μg proteins were resolved under reducing conditions by 12% SDS-PAGE and transferred to nitrocellulose membranes. Following blocking of the blot with 5% non-fat milk in TBS-T buffer (20 mM Tris-HCl, pH 7.6, 137 mM NaCl, 0.2% Tween 20), the anti-Sox4 primary antibody (Chemicon International, cat. #AB5803) was diluted 1:200 (in 1% non-fat milk in TBS-T) and incubated with the blot for 1 hour at room temperature. Next, the filter was washed 3×10 minutes in TBS-T and incubated with the appropriate horseradish peroxidase (HRP)-conjugated secondary antibody for 1 hour at room temperature. Protein bands were revealed by ECL detection. The filter was then stripped and reprobed with anti-actin antibody (Santa Cruz Biotechnology, Heidelberg, Germany, cat. #SC-1616) for normalization.

Proliferation

The procedure was modified from Marzia et al. (Marzia et al., 2000). Briefly, osteoblasts were plated in 24-well multiplates (5000 cells per well) and grown to ~70% confluence. Following incubation for 24 hours in DMEM with antibiotics and 0.2% bovine serum albumin (BSA), the cells were incubated in 1 μCi/ml [^{3}H]thymidine (specific activity 5.0 Ci/mmol; Amersham) overnight. Cells were then washed twice and solubilized in 0.1% SDS. 10 μl 10 mg/ml BSA was added to each sample as a carrier protein, and precipitated by adding 100 μl 100% trichloroacetic acid (TCA) and incubating for 30 minutes on ice. Following centrifugation, the precipitate was resuspended in 0.5 ml 0.1% SDS. 5 ml Insta-Gel II scintillation fluid (Packard Instrument Company, Groningen, The Netherlands) was added and the samples were counted in a β-scintillation counter (Packard Tri-Carb 1900TR).

ALP activity of osteoblasts

Differentiation was evaluated by histochemical and biochemical analyses of ALP activity using reagents and protocols from Sigma kit 104-LS. Total numbers and numbers of ALP-positive cells were mean counts of three microscopic fields from three cultures of WT and *Sox4*$^{+/-}$ mice (magnification 20×). For siRNA experiments (see below), cells were counted from two cultures (two experiments) of WT osteoblasts treated with Sox4 and control siRNA.

Mineralization

Osteoblasts were plated in 6- or 24-well multiplates and grown to 90% confluence (~7 days following plating). Media were then replaced with mineralizing media (DMEM supplemented with 10% FBS, 50 μg/ml ascorbic acid and 10 mM β-glycerophosphate) and cultured for 3 weeks with medium change every 3 days, as described (Marzia et al., 2000). Mineralization was evaluated by von Kossa staining, counting and quantification of positive nodules in 10 representative microscopic fields.

RNA isolation and real-time PCR

Total RNA was isolated from mouse bones and cell cultures using Trizol® (Life Technologies/Invitrogen, MD) and further purified by RNeasy Mini Kit (Qiagen, Hilden, Germany). RNA quality was checked using a Matrix 2100 Bioanalyzer (Matrix AS, Oslo, Norway) and results analyzed by Agilent 2100 expert software (Agilent Technologies, Blacksburg, VA).

1 μg of RNA was subjected to a 20 μl reverse transcriptase (RT) reaction by M-MLV Reverse transcriptase (Promega, Madison, WI) according to the manufacturer's procedure, and diluted 5× before samples (in triplicates) were subjected to real-time PCR analysis in a LightCycler (Roche Diagnostics, Penzberg, Germany). LightCycler™ Fast Start Master SYBR Green (Roche Diagnostics) or Brilliant® SYBR Green QPCR master mix (Stratagene) kits were used. PCR conditions and primer pairs used are listed in Table S1. To distinguish cDNA and genomic DNA, primers were placed on corresponding exons at the junction of an intron. In addition to this, we also used primers for *ALP, Coll1A2* and *PTHR1* as published (Huang et al., 2004), *OCN* (zur Nieden et al., 2003), *c-fos* (Tanaka et al., 2004) and *AP2* (Jiang et al., 2004).

Cycle threshold (Ct) values were obtained graphically (Roche Diagnostics, software version 3.5). Gene expression was normalized to *β-actin* or *GAPDH* and ΔCt values calculated. Comparison of gene expression between two samples (WT and *Sox4*$^{+/-}$ bones or osteoblasts) was obtained by subtraction of ΔCt values between the two samples to give a ΔΔCt value, and relative gene expression calculated as $2^{-\Delta\Delta Ct}$ normalized to WT.

Osteoclast primary cultures

Differentiated primary osteoclasts were obtained from the bone marrow of 5-7-day-old *Sox4*$^{+/-}$ and WT mice by a modification of the method described by David et al. (David et al., 1998; Teti et al., 1999). Pups were sacrificed by cervical dislocation, and long bones were dissected free from soft tissues and cut into small fragments. Bone marrow cells were released by gently pipetting the fragments in DMEM supplemented with 100 IU/ml penicillin, 100 μg/ml streptomycin, 2 mM L-glutamine and 10% FBS. Cells were plated in culture dishes and allowed to attach

for 24 hours before non-adherent cells were removed by aspiration and extensive washing. The total adherent cell fraction was cultured for up to 7 days in the presence of 10^{-8} M 1,25$(OH)_2$vitamin D_3.

Cultures were fixed in 3% paraformaldehyde in 0.1 M cacodylate buffer, and positivity for the osteoclast marker enzyme TRAcP was detected histochemically using the Sigma-Aldrich kit No. 85 (Sigma), according to the manufacturer's instructions.

Osteoclasts were also grown on bone slices, differentiated as described above, and fixed in 3% paraformaldehyde in 0.1 M cacodylate buffer. Cells were then removed by ultrasonication in 1% sodium hypochlorite, and slices were stained with 0.1% toluidine blue. Pits were counted and the pit index computed according to Caselli et al. (Caselli et al., 1997).

RNAi knockdown of gene expression in WT osteoblasts

Four siGENOME™ SMART pool® siRNA duplexes specific for mouse *Sox4* were designed by and purchased from Dharmacon (Lafayette, CO). Osteoblasts from calvariae of 7-day-old WT mice were trypsinized and plated in 24-well plates or in 3.5 cm culture dishes. At approximately 50% confluence, cells were transfected with the annealed siRNA-Sox4 (siRNA final concentration 100 nM) using oligofectamine (Invitrogen, Carlsbad, CA) in Opti-MEM (Invitrogen). Cells were treated with siRNA-Sox4 for 48 hours, then the RNA was extracted, reverse transcribed and subjected to amplification for the *Sox4* gene in order to evaluate its downregulation. The same procedure was followed for RNAi knockdown of *Runx2*.

Statistical analyses

Results are generally expressed as means ± s.d. and analyzed by SPSS v12.0.1. Analyses of bone density time courses were performed using SPSS Mixed Models, taking into account the repeated measurements of each mouse parameter and the dependency of DXA parameters within each individual. Time, genotype and gender were analyzed statistically as fixed effects, with bone area, per cent fat and body mass as covariates for analyses with total BMC and BMD as dependent variables, respectively. Variables obtained from the same bone (DXA-/μCT-results, histomorphometry, biomechanics) were considered as dependent data sets and analyzed by multivariate analyses (MANOVA). Independent data sets were analyzed with unpaired Student's *t*-test, using Welch correction when variances were unequal. For all statistical tests, $P<0.05$ was considered significant.

We are grateful to Hans Clevers for providing the *Sox4*$^{+/-}$ mice for these studies. Thanks to Ole Petter Fraas Claussen and Paula deAngelis for help with flow cytometry, to Åse-Karine Fjeldheim and Ole Kristoffer Olstad for technical advice, and to Joseph Sexton for statistical consulting. D. Pioletti is gratefully thanked for providing resources and guidance for bone biomechanical testing, and for advice regarding evaluation of the results obtained. We are indebted to Fanny Cavat for technical assistance with μCT measurements and Stefania De Grossi and Aileen Murdoch Larsen for technical assistance in histological preparations. The study is part of the EU collaboration Life Sciences, Genomics and Biotechnology for Health OSTEOGENE, project no. 502941. This research has also been supported by a Marie Curie Fellowship of the European Community programme Quality of Life and Management of Living Resources under contract number QLK3-CT-2001-60040 (to R.P. and D.F.), by Helse Øst (project no. 29750104), and by the Norwegian Research Council where S.R. is a research fellow.

References

Ahn, S. G., Kim, H. S., Jeong, S. W., Kim, B. E., Rhim, H., Shim, J. Y., Kim, J. W., Lee, J. H. and Kim, I. K. (2002). Sox-4 is a positive regulator of Hep3B and HepG2 cells' apoptosis induced by prostaglandin (PG)A(2) and delta(12)-PGJ(2). *Exp. Mol. Med.* **34**, 243-249.

Billiard, J., Moran, R. A., Whitley, M. Z., Chatterjee-Kishore, M., Gillis, K., Brown, E. L., Komm, B. S. and Bodine, P. V. (2003). Transcriptional profiling of human osteoblast differentiation. *J. Cell. Biochem.* **89**, 389-400.

Bouxsein, M. L., Pierroz, D. D., Glatt, V., Goddard, D. S., Cavat, F., Rizzoli, R. and Ferrari, S. L. (2005). beta-Arrestin2 regulates the differential response of cortical and trabecular bone to intermittent PTH in female mice. *J. Bone Miner. Res.* **20**, 635-643.

Brodt, M. D., Ellis, C. B. and Silva, M. J. (1999). Growing C57Bl/6 mice increase whole bone mechanical properties by increasing geometric and material properties. *J. Bone Miner. Res.* **14**, 2159-2166.

Caselli, G., Mantovanini, M., Gandolfi, C. A., Allegretti, M., Fiorentino, S., Pellegrini, L., Melillo, G., Bertini, R., Sabbatini, W., Anacardio, R. et al. (1997). Tartronates: a new generation of drugs affecting bone metabolism. *J. Bone Miner. Res.* **12**, 972-981.

Celil, A. B., Hollinger, J. O. and Campbell, P. G. (2005). Osx transcriptional regulation is mediated by additional pathways to BMP2/Smad signaling. *J. Cell. Biochem.* **95**, 518-528.

Critcher, R., Stitson, R. N., Wade-Martins, R., Easty, D. J. and Farr, C. J. (1998). Assignment of Sox4 to mouse chromosome 13 bands A3-A5 by fluorescence in situ hybridization; refinement of the human SOX4 location to 6p22.3 and of SOX20 to chromosome 17p12.3. *Cytogenet. Cell Genet.* **81**, 294-295.

David, J. P., Neff, L., Chen, Y., Rincon, M., Horne, W. C. and Baron, R. (1998). A new method to isolate large numbers of rabbit osteoclasts and osteoclast-like cells: application to the characterization of serum response element binding proteins during osteoclast differentiation. *J. Bone Miner. Res.* **13**, 1730-1738.

De Benedetti, F., Rucci, N., Del Fattore, A., Peruzzi, B., Paro, R., Longo, M., Vivarelli, M., Muratori, F., Berni, S., Ballanti, P. et al. (2006). Impaired skeletal development in interleukin-6-transgenic mice: a model for the impact of chronic inflammation on the growing skeletal system. *Arthritis Rheum.* **54**, 3551-3563.

Dimai, H. P., Linkhart, T. A., Linkhart, S. G., Donahue, L. R., Beamer, W. G., Rosen, C. J., Farley, J. R. and Baylink, D. J. (1998). Alkaline phosphatase levels and osteoprogenitor cell numbers suggest bone formation may contribute to peak bone density differences between two inbred strains of mice. *Bone* **22**, 211-216.

Ducy, P. (2000). Cbfa1: a molecular switch in osteoblast biology. *Dev. Dyn.* **219**, 461-471.

Ferrari, S. L., Pierroz, D. D., Glatt, V., Goddard, D. S., Bianchi, E. N., Lin, F. T., Manen, D. and Bouxsein, M. L. (2005). Bone response to intermittent parathyroid hormone is altered in mice null for {beta}-Arrestin2. *Endocrinology* **146**, 1854-1862.

Gaur, T., Lengner, C. J., Hovhannisyan, H., Bhat, R. A., Bodine, P. V., Komm, B. S., Javed, A., van Wijnen, A. J., Stein, J. L., Stein, G. S. et al. (2005). Canonical WNT signaling promotes osteogenesis by directly stimulating Runx2 gene expression. *J. Biol. Chem.* **280**, 33132-33140.

Giguere, Y. and Rousseau, F. (2000). The genetics of osteoporosis: 'complexities and difficulties'. *Clin. Genet.* **57**, 161-169.

Grant, S. F., Reid, D. M., Blake, G., Herd, R., Fogelman, I. and Ralston, S. H. (1996). Reduced bone density and osteoporosis associated with a polymorphic Sp1 binding site in the collagen type I alpha 1 gene. *Nat. Genet.* **14**, 203-205.

Guo, J., Chung, U. I., Yang, D., Karsenty, G., Bringhurst, F. R. and Kronenberg, H. M. (2006). PTH/PTHrP receptor delays chondrocyte hypertrophy via both Runx2-dependent and -independent pathways. *Dev. Biol.* **292**, 116-128.

Havill, L. M., Rogers, J., Cox, L. A. and Mahaney, M. C. (2006). QTL with pleiotropic effects on serum levels of bone-specific alkaline phosphatase and osteocalcin maps to the baboon ortholog of human chromosome 6p23-21.3. *J. Bone Miner. Res.* **21**, 1888-1896.

Hett, A. K. and Ludwig, A. (2005). SRY-related (Sox) genes in the genome of European Atlantic sturgeon (Acipenser sturio). *Genome* **48**, 181-186.

Hildebrand, T. and Ruegsegger, P. (1997). A new method for the model-independent assessment of thickness in three-dimensional images. *J. Microsc.* **185**, 67-75.

Hong, C. S. and Saint-Jeannet, J. P. (2005). Sox proteins and neural crest development. *Semin. Cell Dev. Biol.* **16**, 694-703.

Huang, J. C., Sakata, T., Pfleger, L. L., Bencsik, M., Halloran, B. P., Bikle, D. D. and Nissenson, R. A. (2004). PTH differentially regulates expression of RANKL and OPG. *J. Bone Miner. Res.* **19**, 235-244.

Hur, E. H., Hur, W., Choi, J. Y., Kim, I. K., Kim, H. Y., Yoon, S. K. and Rhim, H. (2004). Functional identification of the pro-apoptotic effector domain in human Sox4. *Biochem. Biophys. Res. Commun.* **325**, 59-67.

Jepsen, K. J., Akkus, O. J., Majeska, R. J. and Nadeau, J. H. (2003). Hierarchical relationship between bone traits and mechanical properties in inbred mice. *Mamm. Genome* **14**, 97-104.

Jiang, W., Miyamoto, T., Kakizawa, T., Sakuma, T., Nishio, S., Takeda, T., Suzuki, S. and Hashizume, K. (2004). Expression of thyroid hormone receptor alpha in 3T3-L1 adipocytes; triiodothyronine increases the expression of lipogenic enzyme and triglyceride accumulation. *J. Endocrinol.* **182**, 295-302.

Jilka, R. L. (2003). Biology of the basic multicellular unit and the pathophysiology of osteoporosis. *Med. Pediatr. Oncol.* **41**, 182-185.

Johnson, M. L., Harnish, K., Nusse, R. and Van, H. W. (2004). LRP5 and Wnt signaling: a union made for bone. *J. Bone Miner. Res.* **19**, 1749-1757.

Karsenty, G. (1999). The genetic transformation of bone biology. *Genes Dev.* **13**, 3037-3051.

Komori, T., Yagi, H., Nomura, S., Yamaguchi, A., Sasaki, K., Deguchi, K., Shimizu, Y., Bronson, R. T., Gao, Y. H., Inada, M. et al. (1997). Targeted disruption of Cbfa1 results in a complete lack of bone formation owing to maturational arrest of osteoblasts. *Cell* **89**, 755-764.

Kronenberg, H. M. (2006). PTHrP and skeletal development. *Ann. N. Y. Acad. Sci.* **1068**, 1-13.

Lecka-Czernik, B., Moerman, E. J., Grant, D. F., Lehmann, J. M., Manolagas, S. C. and Jilka, R. L. (2002). Divergent effects of selective peroxisome proliferator-activated receptor-gamma 2 ligands on adipocyte versus osteoblast differentiation. *Endocrinology* **143**, 2376-2384.

Lefebvre, V., Li, P. and de Crombrugghe, B. (1998). A new long form of Sox5 (L-Sox5), Sox6 and Sox9 are coexpressed in chondrogenesis and cooperatively activate the type II collagen gene. *EMBO J.* **17**, 5718-5733.

Liu, P., Ramachandran, S., Ali, S. M., Scharer, C. D., Laycock, N., Dalton, W. B., Williams, H., Karanam, S., Datta, M. W., Jaye, D. L. et al. (2006). Sex-determining region Y box 4 is a transforming oncogene in human prostate cancer cells. *Cancer Res.* **66**, 4011-4019.

Lu, X., Gilbert, L., He, X., Rubin, J. and Nanes, M. S. (2006). Transcriptional regulation of the osterix (Osx, Sp7) promoter by tumor necrosis factor identifies

disparate effects of mitogen-activated protein kinase and NF kappa B pathways. *J. Biol. Chem.* **281**, 6297-6306.

Marzia, M., Sims, N. A., Voit, S., Migliaccio, S., Taranta, A., Bernardini, S., Faraggiana, T., Yoneda, T., Mundy, G. R., Boyce, B. F. et al. (2000). Decreased c-Src expression enhances osteoblast differentiation and bone formation. *J. Cell Biol.* **151**, 311-320.

Maschhoff, K. L., Anziano, P. Q., Ward, P. and Baldwin, H. S. (2003). Conservation of Sox4 gene structure and expression during chicken embryogenesis. *Gene* **320**, 23-30.

Mavropoulos, A., Devos, N., Biemar, F., Zecchin, E., Argenton, F., Edlund, H., Motte, P., Martial, J. A. and Peers, B. (2005). sox4b is a key player of pancreatic alpha cell differentiation in zebrafish. *Dev. Biol.* **285**, 211-223.

Mundy, G. R. (2006). Nutritional modulators of bone remodeling during aging. *Am. J. Clin. Nutr.* **83**, 427S-430S.

Nakashima, K., Zhou, X., Kunkel, G., Zhang, Z., Deng, J. M., Behringer, R. R. and de Crombrugghe, B. (2002). The novel zinc finger-containing transcription factor osterix is required for osteoblast differentiation and bone formation. *Cell* **108**, 17-29.

Nguyen, T. V., Livshits, G., Center, J. R., Yakovenko, K. and Eisman, J. A. (2003). Genetic determination of bone mineral density: evidence for a major gene. *J. Clin. Endocrinol. Metab.* **88**, 3614-3620.

Nissen-Meyer, L. S. H., Gautvik, V. T., Reppe, S., Reinholt, F. P., Gautvik, K. M. and Jemtland, R. (2004). Reduced bone mineral density in adult heterozygous Sox4+/– mice. *J. Bone Miner. Res.* Suppl., M038.

Nissen-Meyer, L. S. H., Paro, R., Pedersen, M. E., Fortunati, D., Reppe, S., Brorson, S. H., Gautvik, V. T., Teti, A., Reinholt, F. P., Jemtland, R. et al. (2005). Decreased bone mineral density in adult mice heterozygous for the PHT-regulated transcription factor Sox4 is associated with suppressed osteoblast activity. *J. Bone Miner. Res.* Suppl., SU232.

Parfitt, A. M., Mathews, C. H., Villanueva, A. R., Kleerekoper, M., Frame, B. and Rao, D. S. (1983). Relationships between surface, volume, and thickness of iliac trabecular bone in aging and in osteoporosis. Implications for the microanatomic and cellular mechanisms of bone loss. *J. Clin. Invest.* **72**, 1396-1409.

Parfitt, A. M., Drezner, M. K., Glorieux, F. H., Kanis, J. A., Malluche, H., Meunier, P. J., Ott, S. M. and Recker, R. R. (1987). Bone histomorphometry: standardization of nomenclature, symbols, and units. Report of the ASBMR Histomorphometry Nomenclature Committee. *J. Bone Miner. Res.* **2**, 595-610.

Pittenger, M. F., Mackay, A. M., Beck, S. C., Jaiswal, R. K., Douglas, R., Mosca, J. D., Moorman, M. A., Simonetti, D. W., Craig, S. and Marshak, D. R. (1999). Multilineage potential of adult human mesenchymal stem cells. *Science* **284**, 143-147.

Pramoonjago, P., Baras, A. S. and Moskaluk, C. A. (2006). Knockdown of Sox4 expression by RNAi induces apoptosis in ACC3 cells. *Oncogene* **25**, 5626-5639.

Ralston, S. H. (2002). Genetic control of susceptibility to osteoporosis. *J. Clin. Endocrinol. Metab.* **87**, 2460-2466.

Ralston, S. H. and de Crombrugghe, B. (2006). Genetic regulation of bone mass and susceptibility to osteoporosis. *Genes Dev.* **20**, 2492-2506.

Reppe, S., Rian, E., Jemtland, R., Olstad, O. K., Gautvik, V. T. and Gautvik, K. M. (2000). Sox-4 messenger RNA is expressed in the embryonic growth plate and regulated via the parathyroid hormone/parathyroid hormone-related protein receptor in osteoblast-like cells. *J. Bone Miner. Res.* **15**, 2402-2412.

Reppe, S., Stilgren, L., Olstad, O. K., Brixen, K., Nissen-Meyer, L. S., Gautvik, K. M. and Abrahamsen, B. (2006). Gene expression profiles give insight into the molecular pathology of bone in primary hyperparathyroidism. *Bone* **39**, 189-198.

Schilham, M. W., Oosterwegel, M. A., Moerer, P., Ya, J., de Boer, P. A., van de Wetering, M., Verbeek, S., Lamers, W. H., Kruisbeek, A. M., Cumano, A. et al. (1996). Defects in cardiac outflow tract formation and pro-B-lymphocyte expansion in mice lacking Sox-4. *Nature* **380**, 711-714.

Schilham, M. W., Moerer, P., Cumano, A. and Clevers, H. C. (1997). Sox-4 facilitates thymocyte differentiation. *Eur. J. Immunol.* **27**, 1292-1295.

Schmidt, K., Schinke, T., Haberland, M., Priemel, M., Schilling, A. F., Mueldner, C., Rueger, J. M., Sock, E., Wegner, M. and Amling, M. (2005). The high mobility group transcription factor Sox8 is a negative regulator of osteoblast differentiation. *J. Cell Biol.* **168**, 899-910.

Schriefer, J. L., Robling, A. G., Warden, S. J., Fournier, A. J., Mason, J. J. and Turner, C. H. (2005). A comparison of mechanical properties derived from multiple skeletal sites in mice. *J. Biomech.* **38**, 467-475.

Sekiya, I., Vuoristo, J. T., Larson, B. L. and Prockop, D. J. (2002). In vitro cartilage formation by human adult stem cells from bone marrow stroma defines the sequence of cellular and molecular events during chondrogenesis. *Proc. Natl. Acad. Sci. USA* **99**, 4397-4402.

Shimizu, M., Higuchi, K., Kasai, S., Tsuboyama, T., Matsushita, M., Matsumura, T., Okudaira, S., Mori, M., Koizumi, A., Nakamura, T. et al. (2002). A congenic mouse and candidate gene at the Chromosome 13 locus regulating bone density. *Mamm. Genome* **13**, 335-340.

Tanaka, S., Sakai, A., Tanaka, M., Otomo, H., Okimoto, N., Sakata, T. and Nakamura, T. (2004). Skeletal unloading alleviates the anabolic action of intermittent PTH(1-34) in mouse tibia in association with inhibition of PTH-induced increase in c-fos mRNA in bone marrow cells. *J. Bone Miner. Res.* **19**, 1813-1820.

Teti, A., Taranta, A., Villanova, I., Recchia, I. and Migliaccio, S. (1999). Osteoclast isolation: new developments and methods. *J. Bone Miner. Res.* **14**, 1251-1252.

van de Wetering, M., Oosterwegel, M., van Norren, K. and Clevers, H. (1993). Sox-4, an Sry-like HMG box protein, is a transcriptional activator in lymphocytes. *EMBO J.* **12**, 3847-3854.

Vanky, P., Brockstedt, U., Hjerpe, A. and Wikstrom, B. (1998). Kinetic studies on epiphyseal growth cartilage in the normal mouse. *Bone* **22**, 331-339.

zur Nieden, N. I., Kempka, G. and Ahr, H. J. (2003). In vitro differentiation of embryonic stem cells into mineralized osteoblasts. *Differentiation* **71**, 18-27.

Journal of Cell Science